



ELSEVIER

Catalysis Today 48 (1999) 211–219

CATALYSIS
TODAY

Concomitant use of liquid–liquid batch and continuous plug flow reactors for kinetic model discrimination. Application to the Rh/TPPTS catalysed reduction of the C–C double bond in dimethylitaconate

Claude de Bellefon^{*}, Nathalie Tanchoux, Sylvain Caravieilhès, Daniel Schweich

Laboratoire de Génie des Procédés Catalytiques, CNRS – CPE Lyon, BP 2077, F-69616 Villeurbanne, France

Abstract

The biphasic catalytic reduction of the C–C double bond of dimethylitaconate with a water soluble rhodium/triphenylphosphinetrisulphonated sodium salt (TPPTS) complex is investigated. Kinetic studies in a well-mixed batch reactor provide kinetics parameters and an activation energy of 71 kJ mol^{-1} but cannot discriminate between a first order or a complex kinetic model within the range of substrate concentration where the approximation of linear liquid/liquid partition is respected. Catalytic tests in the centrifugal partition chromatograph (CPC) reactor under steady-state operations in chemical regime and plug flow mode allow discriminating the kinetic models, the complex kinetic rate law being preferred. © 1999 Elsevier Science B.V. All rights reserved.

Keywords: Homogeneous catalysis; Liquid-liquid catalysis; Rhodium; Kinetics; Plug flow reactor; Batch reactor; Model discrimination

1. Introduction

Numerous transition metal complexes based homogeneous catalytic reactions can easily be made biphasic just by functionalisation of the ligands to make the catalyst water soluble [1]. This is currently achieved by sulphonation of phenyl groups which are widely used as organic substituents in phosphines ligands. The Rhône-Poulenc/Ruhr Chemie Process for the hydroformylation of olefins uses a rhodium complex catalyst coordinated with the water soluble

ligand TPPTS. Separation of the product and recovery of the catalyst are thus achieved by simple decantation [2]. However, when using highly sophisticated ligands such as those giving enantioselectivity, the availability and the cost of the catalyst for laboratory studies become the actual drawbacks for a wider application of transition metal complex catalysts. In a previous report, a centrifugal partition chromatograph (CPC) was used as a liquid/liquid continuous catalytic plug flow reactor requiring *low reactional volumes* [3]. However, the test reaction used, the reduction of benzaldehyde to benzyl alcohol, was not of high industrial interest and was rather slow which did not allow working at high conversions. In this report, some new results

^{*}Corresponding author. Fax: +33-04-72-43-16-73; e-mail: cdb@lobivia.cpe.fr

concerning the hydrodynamic and the mass transfer properties of the CPC as well as its use as a catalytic reactor for the liquid/liquid reduction of dimethylitaconate (DMI) into dimethylmethylsuccinate (DMS) will be presented.

2. Experimental

2.1. Chemicals and analysis

The catalyst precursor $[\text{Rh}(\text{cod})\text{Cl}]_2$ (98%, Strem) was used as received. The solvents water and cyclohexane (ACROS) were degassed and purged under argon prior to use but not further purified. TPPTS 30 wt% in water, sodium formate (97%, Aldrich), dimethylitaconate (97%, Aldrich), and decane (99%, Aldrich) were used as received. All the experiments involving the Rh complex were performed under argon or nitrogen. Samples from the catalytic runs were analysed by gas-chromatography on a HP-5790A instrument (Cydex-B SGE capillary column, ca. 25 m, $d=320\text{ }\mu\text{m}$, 2 bar He ml min^{-1} , FID-detector, split injection mode, 1 ml sample intake, internal standard: decane, temperature programme: $80\text{--}100^\circ\text{C}$, $10^\circ\text{C min}^{-1}$; $100\text{--}107^\circ\text{C}$, 1°C min^{-1} ; $107\text{--}230^\circ\text{C}$, $35^\circ\text{C min}^{-1}$, $t(230^\circ\text{C})=1\text{ min}$).

2.2. Partition isotherm measurements

The partition coefficients for DMI and DMS were measured as follows. A solution of DMI (187.7 mg, 1.19 mmol) and decane (143.2 mg, 1.0 mmol) in cyclohexane (20 ml) was mixed with an equal volume of sodium formate in water (5 M, 20 ml, 0.1 mol). After the thermodynamic equilibrium was reached, an analysis of the organic phase was performed. Stepwise addition of DMI up to 240 mg and equilibration provides the partition isotherm for DMI (the partition isotherm of DMS was determined by the same procedure).

2.3. Catalyst preparation

A solution of sodium formate in water (5 M, 24 ml, 120 mmol) was added to an orange slurry of $[\text{Rh}(\text{cod})\text{Cl}]_2$ (148 mg, 0.60 mmol of Rh) and TPPTS 30% in water (7 g, 3.7 mmol). The mixture

was stirred at room temperature for about 12 h and stored at 4°C .

2.4. Catalytic runs in the batch reactor

The apparatus was described in a previous paper [4]. In a typical experiment, the reactor was loaded with an aqueous solution of sodium formate (5 M, 18 ml, 90 mmol) and a mixture of DMI (316 mg, 2.0 mmol) and decane (143.2 mg, 1.0 mmol) in cyclohexane (20 ml). The mixture was then stirred and the temperature was raised up to 40°C (about 20 min) after which time the partition equilibrium was reached. An aliquot of the catalyst (2 ml) prepared as described above was then added. The course of the reaction was followed by analysis of the organic phase by gas-chromatography.

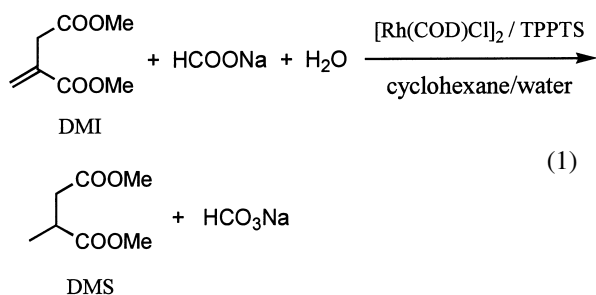
2.5. Catalytic runs in the CPC reactor

The aqueous phase was prepared as follows. An aliquot of the catalyst (8 ml, 15.8 mmol) prepared as described above was added to an aqueous sodium formate solution (5 M, 80 ml, 400 mmol). This aqueous phase was then pumped at 1 ml min^{-1} flow rate into the coiled Teflon tube spinning at 150 rpm. The rotation speed was then set at 800 rpm and cyclohexane was pumped continuously through the coil at 2.5 ml min^{-1} . Some of the stationary aqueous phase was eluted until the hydrodynamic equilibrium was reached in the coil. The volume of the stationary phase in the coil at equilibrium was 50 ml under the conditions studied. The organic solution containing DMI (0.1 kmol m^{-3}) and decane (0.05 kmol m^{-3}) was then pumped through the stationary phase at the desired flow rate. The course of the reaction was followed by analysis of the organic phase at the CPC outlet.

3. Results and discussion

3.1. Reaction

The test reaction is the reduction of DMI to DMS with sodium formate, catalysed by a water soluble Rh complex [5]:



Analysis of the organic layer and mass balance calculations confirm the total (>95%) conversion of the substrate DMI into the product DMS. The side product (<5%) is an isomer of DMI, the 2-dimethyl-mesaconate (DMM), formed by the shift of the double bond from the external to the internal position. Such an isomerisation of terminal olefins to internal has been frequently reported as a side reaction in the case of, e.g., hydrogenation [6].

3.2. Liquid–liquid partition equilibrium

Because the catalyst is located in the aqueous layer, the organic reagent DMI should first transfer from the organic to the aqueous phase. Similarly, the product DMS should transfer from the aqueous phase where it forms to the organic phase. The course of the reaction being more conveniently followed by analysis of the organic layer, it is of importance to correlate that measured concentration to the concentration in the aqueous phase where the catalytic reaction actually takes place. The concentration of species A in the organic and the aqueous phase was described by the linear relationship:

$$P_A = \frac{C_{\text{Org}}^A}{C_{\text{Aq}}^A} (m_{\text{Aq}}^3 m_{\text{Org}}^{-3}).$$

It is well known that the thermodynamic equilibrium in the case of ternary mixtures cannot be described properly for all the range of composition by a constant partition factor P_A . However, in the case of the ternary system described here and for the range of concentrations used, this linear relation is valid. The partition of the substrate DMI between the organic and the aqueous phase was measured for several formate concentrations at 25°C (Fig. 1). The partition coeffi-

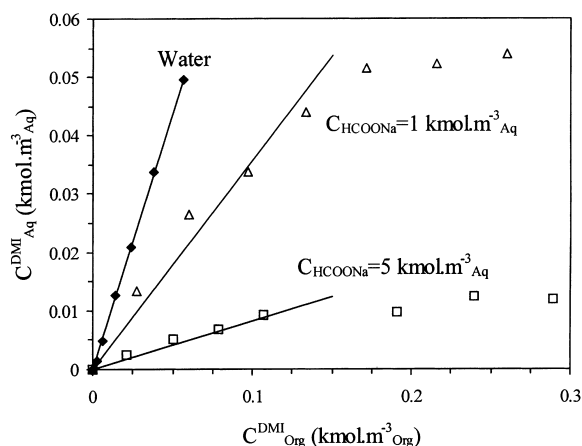


Fig. 1. Partition isotherms (293 K) of dimethylitaconate (DMI) in pure water and in sodium formate solutions.

cients P_A are computed from the experimental isotherms (Table 1).

Because the catalytic reaction was run between 303 and 333 K, the effect of temperature on the partition coefficient was checked. As pointed in Section 2, the procedure for a catalytic test involves first the thermodynamic equilibration of the liquid phases prior to the addition of the catalyst. The measured concentrations in the organic layer after equilibration and before reaction provide data which conform the linear partition model. This is well demonstrated in the parity diagram of Fig. 2 in which the measured DMI concentration in the organic layer is plotted vs. the concentration given by the linear approximation:

$$C_{\text{Org}}^{\text{DMI}} = \frac{\alpha P_{\text{DMI}} n_{\text{DMI}}}{(1 + \alpha P_{\text{DMI}}) V_{\text{Org}}}, \quad (2)$$

where n_{DMI} is the molar quantity of DMI in the experiment, α the liquid phases volumic ratio ($m_{\text{Org}}^3 m_{\text{Aq}}^{-3}$), P_{DMI} the DMI partition coefficient and V_{Org} is the volume of the organic layer. This result

Table 1
Cyclohexane/water partition coefficients of DMI and DMS for various sodium formate concentrations at 293 K^a

C_{HCOONa} (kmol m ⁻³ _{Aq})	0	1	2.5	5
P_{DMI} (m ³ _{Aq} m ⁻³ _{Org})	1.2	2.8	4.3	11.3
P_{DMS} (m ³ _{Aq} m ⁻³ _{Org})	1.7	4	5.6	14

^a A linear partition is observed for $0 \leq C_{\text{Org}}^{\text{DMI}} \leq 0.13 \text{ kmol m}^{-3}$.

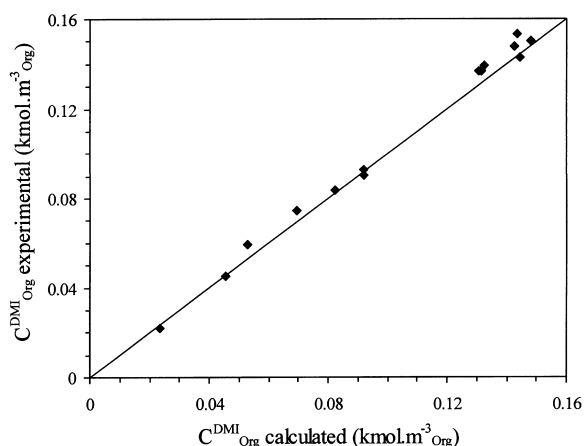


Fig. 2. Calculated vs. experimental $C_{\text{Org}}^{\text{DMI}}$ at thermodynamic equilibrium.

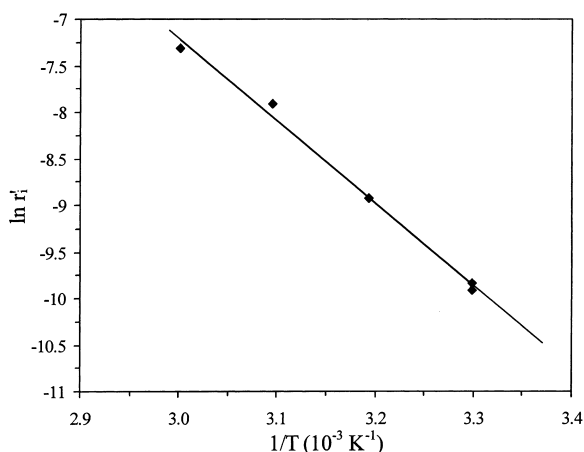


Fig. 3. Arrhenius plot of the observed initial rate of reaction r'_i ($C_{\text{Org}0}^{\text{DMI}} = 0.1 \text{ kmol m}^{-3}$, $C_{\text{Aq}}^{\text{Rh}} = 0.002 \text{ kmol m}^{-3}$, $\alpha=1$).

evidences the weak influence of the temperature on the partition coefficient within the range of temperatures used in the work.

3.3. Kinetic studies of the reaction in a well-mixed batch reactor

Chemical regime in the well-mixed batch reactor at 1100 rpm was first checked [4]. Addition of the side product DMM to the reaction mixture does not influence the rate of reaction. Addition of the main products DMS and sodium hydrogenocarbonate also has no influence on the course of the reaction.

The influence of the temperature was measured. Arrhenius plot of the observed initial rate of reaction r'_i provided an activation energy of 71 kJ mol^{-1} (Fig. 3). This value is in agreement with those reported for other hydrogen transfer reductions of olefins [7].

The observed initial rate dependence on the initial concentration of the substrate $C_{\text{Org}0}^{\text{DMI}}$ is shown in Fig. 4. Neither a simple first-order model nor a more complex kinetic model can properly adjust the data. This may be due to poorly defined initial conditions or to the difficulties to actually determine the values of r'_i , two problems that are typical of batch kinetics measurements. The inconveniences of kinetic parameter estimation based on initial rates of reaction have been debated [8]. Both because complex or first-order kinetics have been reported for similar reactions [9]

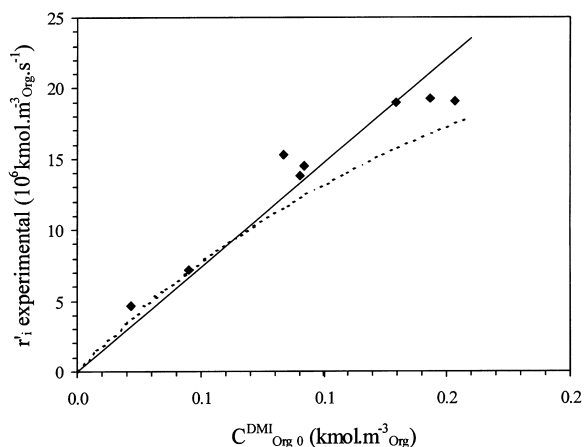


Fig. 4. Influence of the substrate concentration on the observed initial rate of reaction r'_i (313 K, $C_{\text{Aq}}^{\text{Rh}} = 0.002 \text{ kmol m}^{-3}$, $\alpha = 1$). Experimental (symbols): complex model (—); first-order model (---).

and to account for all the observations found during that preliminary studies, two semi-empirical rate models are proposed:

first-order kinetic model :

$$r_{\text{Aq}} = k C_{\text{Aq}}^{\text{Rh}} C_{\text{Aq}}^{\text{DMI}} \quad (\text{kmol m}^{-3} \text{ s}^{-1}), \quad (3)$$

complex kinetic model :

$$r_{\text{Aq}} = \frac{k C_{\text{Aq}}^{\text{Rh}} C_{\text{Aq}}^{\text{DMI}}}{K C_{\text{Aq}}^{\text{DMI}} + 1} \quad (\text{kmol m}^{-3} \text{ s}^{-1}). \quad (4)$$

The DMI concentration being measured in the organic phase, the rate is more conveniently expressed with respect to $C_{\text{Org}}^{\text{DMI}}$. Knowing that $n_{\text{DMI}} = n_{\text{Aq}}^{\text{DMI}} + n_{\text{Org}}^{\text{DMI}}$ and from the mass balance in the batch reactor, it comes:

$$\text{first-order kinetic model : } -\frac{dC_{\text{Org}}^{\text{DMI}}}{dt} = r' = \frac{kC_{\text{Aq}}^{\text{Rh}}}{1 + \alpha P_{\text{DMI}}} C_{\text{Org}}^{\text{DMI}} \quad (\text{kmol m}_{\text{Org}}^{-3} \text{ s}^{-1}), \quad (5)$$

$$\text{complex kinetic model : } -\frac{dC_{\text{Org}}^{\text{DMI}}}{dt} = r' = \frac{kC_{\text{Aq}}^{\text{Rh}}}{1 + \alpha P_{\text{DMI}} (K/P_{\text{DMI}}) C_{\text{Org}}^{\text{DMI}} + 1} C_{\text{Org}}^{\text{DMI}} \quad (\text{kmol m}_{\text{Org}}^{-3} \text{ s}^{-1}). \quad (6)$$

The kinetic studies performed in the range of conditions given in Table 2 provided concentration vs. time profiles from which the kinetic parameters can be extracted. This is done by using a kinetic parameter estimation software able to perform numerical integrations using the concentration vs. time profiles [8]. Figs. 5 and 6 compare the experimental results and those obtained from the optimal parameters.

As evidenced in Fig. 5, both kinetic models fit rather well the experimental concentration vs. time profiles for six experiments at different DMI concentration and different liquid phase volume ratio ($\alpha=1, 0.5$ and 0.2) at 313 K and constant catalyst loading ($C_{\text{Aq}}^{\text{Rh}} = 0.002 \text{ kmol m}^{-3}$). The result of the kinetic parameters estimation and their confidence intervals is presented in Table 3. A parity

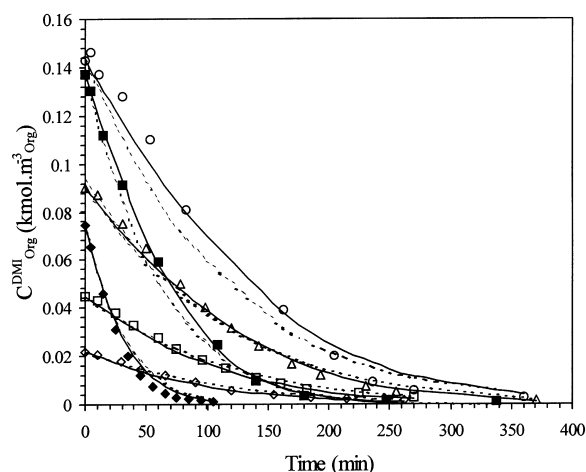


Fig. 5. Concentration vs. time profiles. Experimental (symbols): complex model (—); first-order model (---).

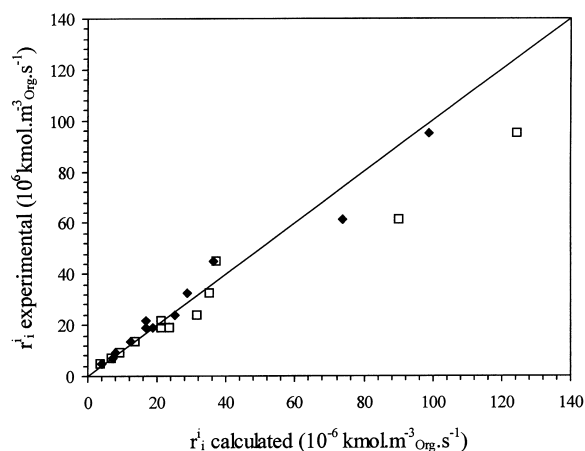


Fig. 6. Calculated vs. experimental initial rate of reaction: complex model (◆); first-order model (□).

Table 2
Range of conditions for kinetic study in batch reactor

Concentration of catalyst ($\text{kmol m}_{\text{Aq}}^{-3}$)	0.0018–0.005
Temperature (K)	303–313–323–333
Organic phase solvent	Cyclohexane
Initial concentration of DMI in the organic phase ($\text{kmol m}_{\text{Org}}^{-3}$)	0.024–0.144
Initial concentration of DMI in the aqueous phase ($\text{kmol m}_{\text{Aq}}^{-3}$)	0.0021–0.013
Stirring speed (rpm)	1100
Aqueous phase volume (10^{-6} m^3)	20–100
Organic phase volume (10^{-6} m^3)	10–20
Volume ratio α ($\text{m}_{\text{Org}}^3 \text{ m}_{\text{Aq}}^{-3}$)	0.2–1

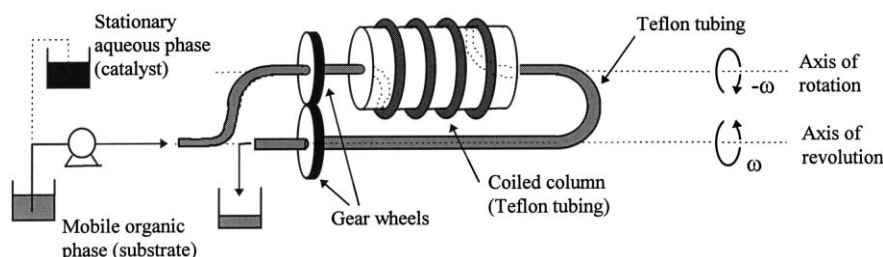
plot of the calculated vs. experimental initial rate of reaction r'_i indicates that the complex kinetic model seems to better account for all the batch experiments (Fig. 6).

Knowing the intrinsic kinetics, the reaction was studied in the CPC in order to: (i) determine which process could be limiting in that new continuous reactor, and (ii) help to discriminate between the two kinetic models.

Table 3

Estimated kinetic constants and statistical analysis for the kinetic models

	k ($\text{m}^3_{\text{Aq}} \text{kmol}^{-1} \text{s}^{-1}$)		K ($\text{m}^3_{\text{Aq}} \text{kmol}^{-1}$)		WRSS ^b
	Value	Confidence interval ^a	Value	Confidence interval ^a	
First-order model	0.87	0.83–0.90	—	—	69
Complex model	1.12	1.08–1.13	63	45–79	28

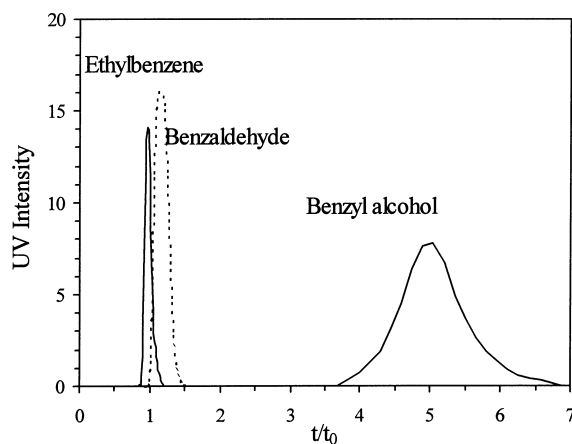
^aInterval at 95% confidence level.^bWRSS=weighted residual sum of squares.Fig. 7. Schematic representation of the CPC. Volume, length and inner diameter of the column: $55 \cdot 10^{-6} \text{ m}^3$, 26.5 m and $1.63 \cdot 10^{-3} \text{ m}$. Speed of revolution 800 rpm.

3.4. Hydrodynamics and mass transfer in the centrifugal partition chromatograph

The CPC used in this study has been described in detail [3,10,11]. A schematic representation of the apparatus is given in Fig. 7.

The hydrodynamic properties and mass transfer capability of the CPC were studied from residence time distribution analysis (RTD) [12]. Ethylbenzene was used as the inert tracer since it is not soluble in the catalytic phase. The determination of the characteristic time for mass transfer t_m between the organic mobile phase and the aqueous catalytic stationary phase was made with benzaldehyde and benzyl alcohol. A typical RTD profile is shown in Fig. 8. Performing the experiments at different flow rates reveals that t_m is proportional to the reciprocal of the flow rate (Fig. 9).

Assuming that the values of t_m for DMI and DMS would not be too different from those obtained with benzaldehyde and benzyl alcohol, and extrapolating the linear correlation $t_m = f(1/Q)$ to lower flow rates ($2 \cdot 10^{-9} \text{ m}^3 \text{s}^{-1}$) provides t_m values lying between 10 and 200 s. For the chemical reaction, a characteristic reaction time of $t_r = 700 \text{ s}$ may be computed as the

Fig. 8. Typical RTD profile. t =retention time of the tracers; t_0 =mean residence time of the mobile phase.

reciprocal of the observed kinetic constant for the fastest reaction run in the batch reactor (at 313 K). Although comparison of t_m and t_r reveals that the limiting process in the CPC reactor with this new reaction should be the chemical reaction, these characteristic times are close enough to check for mass transfer limitations while operating in the CPC.

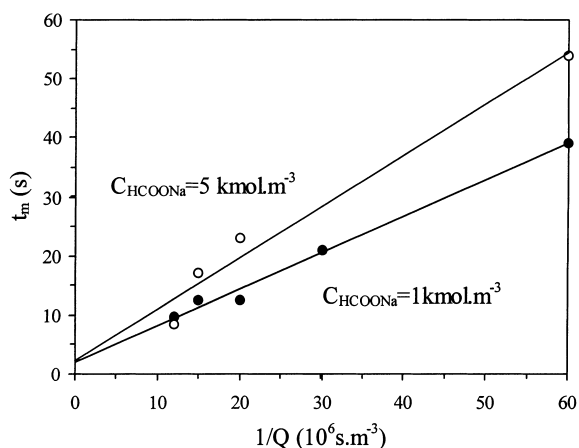


Fig. 9. Determination of t_m at different flow rates for two different concentrations of sodium formate.

3.5. Reaction in the centrifugal partition chromatograph

The catalyst was checked for deactivation in the CPC. In an experiment (800 rpm, 320 K, $Q=17 \cdot 10^{-9} \text{ m}^3 \text{ s}^{-1}$, $C_{\text{Aq}}^{\text{Rh}} = 0.002 \text{ kmol m}^{-3}$, $C_{\text{Org}}^{\text{DMI}} = 0.1 \text{ kmol m}^{-3}$), the reaction was conducted for up to 2 h in the CPC without decrease in the experimental conversion (55%). Furthermore, after running tests in the CPC, the catalytic phase was collected and tested in the batch reactor to check for catalyst deactivation. In no case decreases in the catalyst performances were observed. This confirmed that formate consumption by the reaction (typically 2–5%) has a negligible effect on the kinetics.

Assuming plug flow with no axial dispersion and no mass transfer limitations, the steady-state conversions are:

first-order kinetic model :

$$\chi_{\text{calculated}} = 1 - e^{k C_{\text{Aq}}^{\text{Rh}} V_{\text{Aq}} / P_{\text{DMI}} Q_{\text{Org}}}, \quad (7)$$

complex kinetic model : $\ln(1 - \chi_{\text{calculated}})$

$$-\frac{K}{P_{\text{DMI}}} C_{\text{Org}}^{\text{DMI}} \chi_{\text{calculated}} = -\frac{k C_{\text{Aq}}^{\text{Rh}} V_{\text{Aq}}}{P_{\text{DMI}} Q_{\text{Org}}}. \quad (8)$$

Two operating parameters have been varied: the flow rate and the inlet substrate concentration (Table 4). The influence of the flow rate on the experimental conversion measured at the outlet of

Table 4

Range of conditions for the experiments in the CPC reactor

Concentration of catalyst ($\text{kmol m}_{\text{Aq}}^{-3}$)	0.0018
Inlet concentration of DMI ($\text{kmol m}_{\text{Org}}^{-3}$)	0.05–0.13
Aqueous phase volume ($10^{-6} \text{ m}_{\text{Aq}}^3$)	50
Volume of the CPC reactor (10^{-6} m^3)	55
Volume ratio α ($\text{m}_{\text{Org}}^3 \text{ m}_{\text{Aq}}^{-3}$)	0.1
Organic mobile phase flow rate ($10^{-9} \text{ m}^3 \text{ s}^{-1}$)	7–26
Speed of revolution (rpm)	780–820

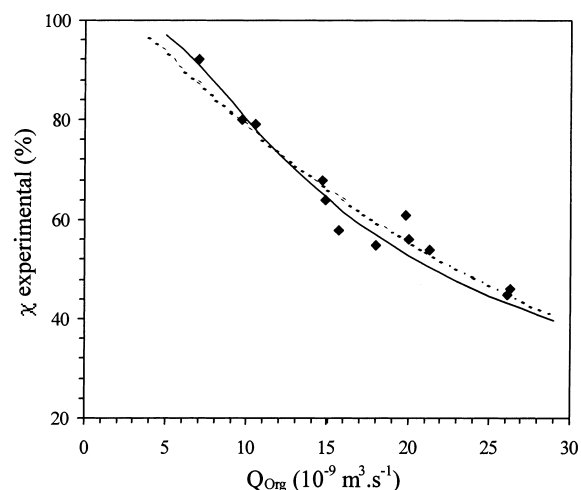


Fig. 10. Conversion vs. flow rate in the CPC: experimentals (◆); complex model (—); first-order model (---).

the CPC is shown in Fig. 10. Both kinetic models fit rather well the experimental data. While this set of experiments cannot help to discriminate between the two kinetic models, it indicates the limiting process in the CPC, i.e. the chemical regime, since no mass transfer limitations are required to account for the experimental data (Fig. 11).

Note that the intrinsic kinetic constants at the temperature of the experiments in the CPC has been computed with the activation energy value found above. In the case of the complex model, the influence of the temperature on the inhibition constant K has been neglected. This is supported by previous reports which have found little effect of the temperature on similar inhibition constants in, e.g., the hydroformylation of olefins [13].

The influence of the substrate concentration is depicted in Fig. 12. From this set of experiments, the model involving a complex kinetic behaviour is

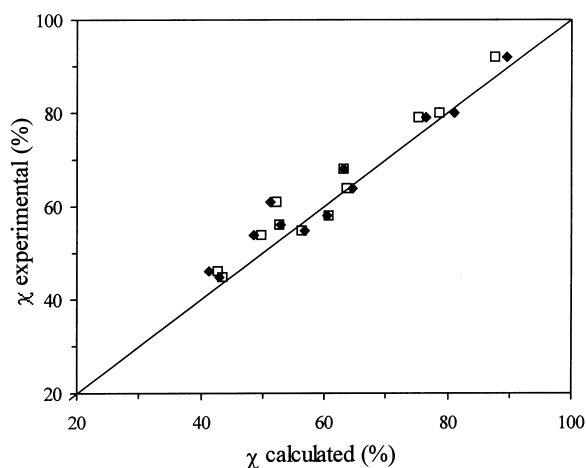


Fig. 11. Calculated vs. experimental conversion: complex model (◆); first-order model (□).

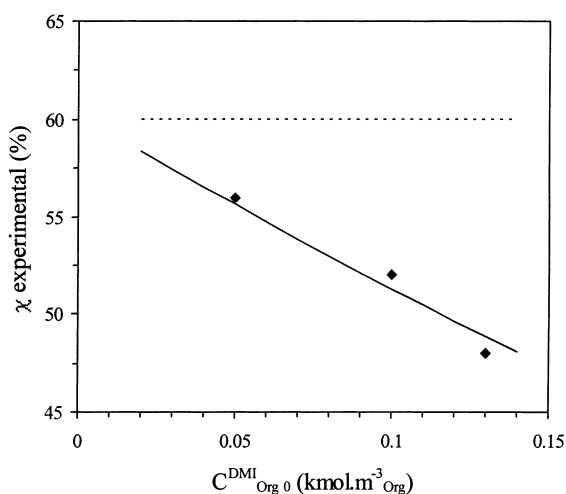


Fig. 12. Influence of the substrate inlet concentration on the conversion in the CPC at 320 K: experimentals (◆); complex model (—); first-order model (---).

chosen since a first-order rate law model would have predicted a constant conversion under these conditions in a plug flow reactor.

4. Conclusion and future works

The use of the CPC reactor as a tool for helping in kinetic models discrimination has been presented. For the catalytic reduction of dimethylitaconate into

dimethylmethylsuccinate in a two-phase system, a complex kinetic model including inhibition by the substrate is validated. In the centrifugal partition chromatograph reactor, while it was expected from both the batch experiments and the residence time distribution analysis that the limiting process could be the mass transfer, it is demonstrated that the CPC was actually operating under chemical regime. Thus, in order to better evaluate the mass transfer capability of this new reactor, much faster reactions should be tested. The possible influence of the rotation speed in the CPC on the mass transfer process is under current investigation. Finally, the CPC has been used only under steady-state conditions up to now. Future works will be devoted to use the chromatographic properties of the CPC, i.e. in the transient or pulse mode.

5. Notations

C_{Org}^{DMI}	concentration of species DMI in the organic phase (kmol m_{Org}^{-3})
$C_{Org 0}^{DMI}$	concentration of DMI in the organic phase (kmol m_{Org}^{-3}) at t_0 in the batch reactor
$C_{Org i}^{DMI}$	concentration of DMI in the organic phase (kmol m_{Org}^{-3}) at the CPC inlet
C_{Aq}^{DMI}	concentration of species DMI in the aqueous phase (kmol m_{Aq}^{-3})
C_{Aq}^{Rh}	concentration of Rh in the aqueous phase (kmol m_{Aq}^{-3})
k	intrinsic reaction rate constant ($\text{m}_{Aq}^3 \text{ kmol}^{-1} \text{ s}^{-1}$)
n_{Org}^{DMI}	number of moles of DMI in the organic phase (mol)
n_{Aq}^{DMI}	number of moles of DMI in the aqueous phase (mol)
P_{DMI}	partition coefficient of DMI between the organic and the catalytic phase ($\text{m}_{Aq}^3 \text{ m}_{Org}^{-3}$)
P_{DMS}	partition coefficient of DMS between the organic and the catalytic phase ($\text{m}_{Aq}^3 \text{ m}_{Org}^{-3}$)
Q_{Org}	flow rate of the mobile organic phase ($\text{m}_{Org}^3 \text{ s}^{-1}$)
r_{Aq}	rate of the reaction per unit volume of the aqueous catalytic phase ($\text{kmol m}_{Aq}^{-3} \text{ s}^{-1}$)
r'	observed rate of the reaction per unit volume of the organic phase ($\text{kmol m}_{Org}^{-3} \text{ s}^{-1}$)
t_m	characteristic time for mass transfer between the two liquid phases (s)

TPPTS	triphenylphosphinetrisulphonated, sodium salt
t_r	characteristic time for the chemical reaction (s)
V_{Aq}	volume of the aqueous phase (m_{Aq}^3)
V_{Org}	volume of the organic phase (m_{Org}^3).
α	volumic ratio of the organic phase and the aqueous phase ($m_{Org}^3 m_{Aq}^{-3}$)
χ	molar conversion (dimensionless)

Acknowledgements

The authors are grateful to the Région Rhône-Alpes, the CNRS and the Ecole de Chimie Physique Electronique de Lyon (CPE Lyon) for financial support.

References

- [1] B. Cornils, W.A. Herrmann, I.T. Horvath, P. Panster, S. Wieland, in: B. Cornils, W.A. Herrmann (Eds.), *Applied Homogeneous Catalysis with Organometallic Compounds*, VCH, Weinheim, 1996, pp. 575–605.
- [2] B. Cornils, E. Kuntz, J. Organomet. Chem. 502 (1995) 177–186.
- [3] C. de Bellefon, S. Caravieilhès, C. Joly-Vuillemin, D. Schweich, A. Berthod, Chem. Eng. Sci. 53 (1998) 71–74.
- [4] C. de Bellefon, N. Tanchoux, S. Caravieilhès, J. Organomet. Chem., (1998) 143–150.
- [5] D. Sinou, M. Safi, J. Mol. Catal. A 68 (1991) L9–L12.
- [6] I. Hablot, J. Jenck, G. Casamatta, H. Delmas, Chem. Eng. Sci. 47 (1992) 2689–2694.
- [7] R.A.W. Johnstone, A.H. Wilby, Chem. Rev. 85 (1985) 129–170.
- [8] C. Joly-Vuillemin, D. Gavroy, G. Cordier, C. de Bellefon, H. Delmas, Chem. Eng. Sci. 49 (1994) 4839–4849.
- [9] M. Baerns, P. Claus, in: B. Cornils, W.A. Herrmann (Eds.), *Applied Homogeneous Catalysis with Organometallic Compounds*, VCH, Weinheim, 1996, p. 686.
- [10] Y. Ito, J. Chromatogr. 538 (1991) 3–25.
- [11] A. Berthod, M. Bully, Anal. Chem. 63 (1991) 2508–2512.
- [12] J. Villermaux, J. Chromatogr. 406 (1987) 11–26.
- [13] R.M. Deshpande, R.V. Chaudhari, Ind. Eng. Chem. Res. 27 (1988) 1996–2002.